Plasma Physics and Controlled Fusion, Vol. 34, No. 7, pp. 1173 to 1183, 1992
Printed in Great Britain.

0741–3335/92 $5.00+ .00

RECONSTRUCTION OF PLASMA EDGE DENSITY PROFILES FROM LiI(2s–2p) EMISSION PROFILES

J. SCHWEINZER
Max-Planck-Institut für Plasmaphysik, D-8046 Garching bei München, Germany

E. WOLFRUM, F. AUMAYR, M. PÖCKL and H. WINTER
Institut für Allgemeine Physik, TU Wien, Wiedner Hauptstr. 8–10, A-1040 Wien, Austria

R. P. SCHORN and E. HINTZ
Institut für Plasmaphysik der KFA Jülich GmbH, Association EURATOM/KFA, Postfach 1913, D-5170 Jülich, Germany

and

A. UNTERREITER
TU Berlin, Fachbereich 3/Mathematik, Straße d. 17. Juni 136, D-1000 Berlin, Germany

(*Received* 30 *December* 1991; *and in revised form* 2 *March* 1992)

Abstract—The injection of 10–100 keV Li^0 diagnostic beams into magnetically confined fusion plasmas causes collisionally induced LiI emission at 670.8 nm, in close relation to the edge plasma electron density. A numerical method for quantitative reconstruction of the plasma density exclusively from relative LiI 670.8 nm emission profiles as measured along the diagnostic beam has been developed, involving all relevant collisional interactions of the Li atoms with plasma constituents. The applicability of the described algorithm is illustrated by experimental results obtained for the TEXTOR Tokamak edge plasma at KFA Jülich.

1. INTRODUCTION

THE DETERMINATION of space- and time-resolved electron density profiles in the edge region of magnetically confined fusion plasmas is of great interest for a more detailed understanding of plasma–wall interaction. Conventional methods such as electrical probes, passive photon spectroscopy, laser scattering or interferometric techniques encounter serious restrictions concerning their applicability and achievable resolution in the spatially rather limited and inhomogeneous boundary layer plasmas.

By injection of atomic Li beams into the plasma, several of these difficulties can be overcome. Li beam methods are based on measuring the LiI(2s–2p) resonance line at 670.8 nm, which becomes excited due to collisions of the injected Li atoms with plasma particles. Therefore, the resulting line emission intensity is connected to the plasma density. Thermal as well as superthermal (laser blow off) Li diagnostic beams have successfully been used at TEXTOR (POSPIESZCZYK and ROSS, 1988a, b; POSPIESZCZYK *et al.*, 1989) as well as other plasma devices (KADOTA *et al.*, 1982; IGUCHI *et al.*, 1985), but because of strong beam attenuation they are limited to the outermost plasma region (the "scrape off layer/SOL"). In order to increase the penetration depth of the probing Li atoms, beam sources with keV injection energy have been installed, e.g. at ASDEX [60 keV/0.5 mA (MCCORMICK *et al.*, 1984, 1985)] and TEXTOR [20 keV/5 to 10 mA (POSPIESZCZYK *et al.*, 1989; SCHORN *et al.*, 1991, 1992)].

In the case of Li beams with energies well below a few hundred electronvolts, the

beam attenuation and LiI line emission can simply be modelled by considering the Li(2s) groundstate, the Li(2p) excited state and electron impact processes only (POSPIESZCZYK *et al.*, 1989). However, data evaluation becomes a considerably more complicated task for keV Li beams (SCHORN *et al.*, 1991).

In the edge plasma the fast Li atoms interact not only with electrons, but also with hydrogen and impurity ions, and consequently become excited as well as ionized via related collisional processes (impact excitation, ionization and charge exchange). Furthermore, such excited LiI states undergo radiative and collisional de-excitation (for fast beams collisional de-excitation becomes important in plasma regions with higher electron densities), and the effective lifetimes of excited states tend to smear out structures in the electron density. A sufficiently correct data evaluation therefore has to assume that the occupation number for the Li(2p) state [which is proportional to the Li(2s–2p) photon intensity at 670.8 nm], the plasma density and the occupation numbers of other Li(nl) states are interrelated by a system of coupled differential equations (cf. SCHORN *et al.*, 1991). We have developed a recursive algorithm to reconstruct the plasma electron density exclusively from relative scans of the LiI 670.8 nm emission intensity along the diagnostic beam direction. In principle, our method can fully recover spatial variations in electron density, independently of smearing-out effects resulting from the effective lifetimes as mentioned above.

The description of this method is given in Section 2, and examples of edge electron density profiles measured in this way at the Tokamak experiment TEXTOR at KFA Jülich are presented and compared with other, independent diagnostic data in Section 3, showing the principal advantages of the presented new method as well as its limitations.

2. DESCRIPTION OF THE RECONSTRUCTION ALGORITHM

We give only a short presentation of the developed reconstruction method, since a more detailed mathematical description of the applied numerical algorithm and the also needed rate coefficients for the various involved collision processes will be given elsewhere.

The time evolution of the fast Li beam composition (i.e. of the occupation numbers of various Li states) as seen by an observer moving with the injected Li atoms, can be decribed by a system of coupled differential equations (SCHORN *et al.*, 1991). If a local plasma coordinate z along the injected Li beam ($z = 0 \ldots$ entrance of the Li beam into the plasma) is introduced as the independent variable, the rate equations for the occupation numbers $N_i(z)$ of the neutral Li states [$i = 1$ denotes Li(2s), $i = 2$ denotes Li(2p), and so on] and the boundary conditions are given by equations (1a, b), respectively, using the Einstein sum convention further on. The density of each plasma component has to be expressed by the electron density n_e, which for impurity-free plasmas means $n_p = n_e$, whereas inclusion of impurity ions will be discussed below.

$$\frac{dN_i(z)}{dz} = [n_e(z)a_{ij}(T(z)) + b_{ij}]N_j(z) \tag{1a}$$

$$N_i(z = 0) = \delta_{1i}. \tag{1b}$$

The coefficients a_{ij} $(i \neq j)$ in the rate equations cover excitation and de-excitation processes for the Li atoms from state j to state i due to collisions with electrons and protons of the plasma, respectively. Attenuation of the Li state i because of its ionization in collisions with plasma particles and excitation as well as de-excitation to any other bound states j are included in the coefficients a_{ii}.

$$a_{ii} \leqslant 0\,; \quad a_{ij} \geqslant 0,\ i \neq j. \tag{2}$$

For our calculations the knowledge of cross-sections or the related rate coefficients for collision processes of the various plasma particles with Li in all states considered is required. These rate coefficients depend on the beam velocity and the electron temperature $T_e(z)$ (SCHORN *et al.*, 1991). Since processes of Li atoms with protons only weakly depend on the proton temperature (AUMAYR and WINTER, 1985), the latter in good approximation has been set to be equal to T_e. In test calculations the results have been found to be insensitive to proton temperature variations by more than a factor of 2.

Spontaneous emission processes are described by coefficients b_{ij}, which are evaluated from tabulated values for transition probabilities of excited atomic Li states (WIESE *et al.*, 1969).

For any given density $n_e(z)$ the initial value problem according to equations (1a, b) can easily be solved within a standard "variable step–variable order" Adams method (NAG, 1984). For illustration, a linearly increasing electron density profile has been assumed to calculate occupation numbers of the five most tightly bound Li states as shown in Fig. 1. Inclusion of more bound Li states ($n \geqslant 4$) into the calculations has been tested and found to be unnecessary.

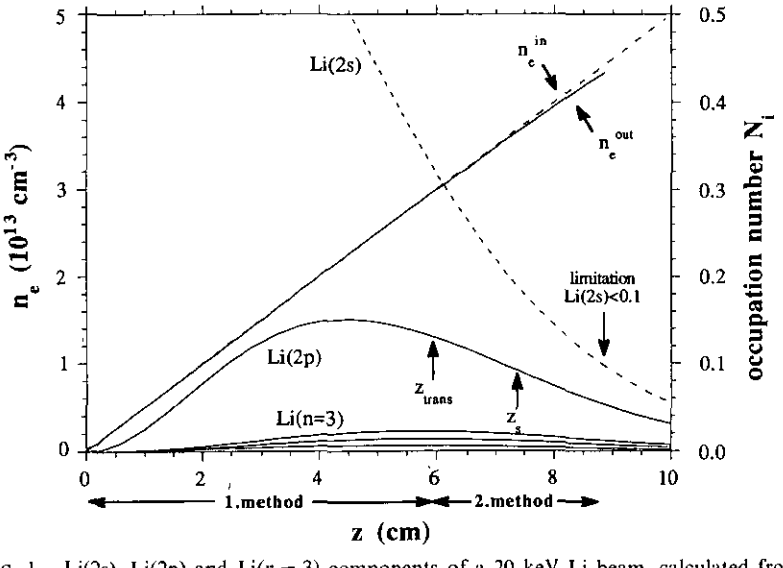

FIG. 1.—Li(2s), Li(2p) and Li($n = 3$) components of a 20 keV Li beam, calculated from an assumed linearly increasing electron density n_e^{in}. The resulting Li(2p) profile has been used to reconstruct the electron density n_e^{out}. z_s indicates the position of the singularity. From z_{trans} onward the second method has been used (for further explanation see text).

The measured emission profile $\mathrm{Li}_{2p}(z)$, which is delivered from the Li beam diagnostic setup, is directly related to the occupation number $N_2(z)$ of the Li(2p) state.

$$\alpha \mathrm{Li}_{2p}(z) = N_2(z) \quad \alpha = \text{const.} \tag{3}$$

In the following, the proportionality constant α will be assumed to be already known, with its actual determination being described later on. We have to solve the inverse problem of finding the coefficient function $n_e(z)$ according to equation (1a), where only one component $\alpha \mathrm{Li}_{2p}(z)$ of the solution vector **N** (components N_i) is known. Two numerical methods, i.e. a one-step and a multi-step method, have been developed for the determination of these density profiles. Both methods together permit the evaluation of the complete density profile by integration of the rate equations in the range $[z = 0, z_L]$, with z_L defined as that beam position where the occupation number $N_1(z_L) = 0.1$. Calculations must be terminated for $z > z_L$ because of dramatically increasing errors in reconstruction.

Equation (4) has been derived for the determination of $n_e(z)$ by algebraic rearrangement of the integrated second equation of the system of coupled equations (1a), with h being a small quantity.

$$n_e(z) \approx \frac{\alpha(\mathrm{Li}_{2p}(z+h) - \mathrm{Li}_{2p}(z)) - \alpha b_{22} \int_z^{z+h} \mathrm{Li}_{2p}(s)\,\mathrm{d}s - h b_{2j''} N_{j''}(z)}{\alpha \int_z^{z+h} a_{22}(s) \mathrm{Li}_{2p}(s)\,\mathrm{d}s + \int_z^{z+h} a_{2j'}(s)\,\mathrm{d}s\, N_{j'}(z)} \tag{4}$$

$$j' \equiv j \neq 2, \quad j'' \equiv j > 2.$$

By stepwise integration of (1a) starting at $z = 0$ and making use of equation (4), the electron density profile of interest is delivered.

However, this method for evaluating the density can only be applied as long as the denominator of the above equation does not change its sign during integration. Unfortunately, this may happen at some coordinate "z_s", because of the properties of the coefficients a_{ij}, see equation (2).

For "reasonable" n_e profiles both the denominator and the numerator in equation (4) have to change sign simultaneously at the same z coordinate. Neglecting only weakly populated Li($n > 2$) states, a good estimate for z_s can be obtained by solving equation (5) before any integration of the rate equation is performed.

$$0 = \alpha\left(\mathrm{Li}_{2p}(z+h) - \mathrm{Li}_{2p}(z) + |b_{22}| \int_z^{z+h} \mathrm{Li}_{2p}(s)\,\mathrm{d}s\right) = \frac{\mathrm{d}\mathrm{Li}_{2p}}{\mathrm{d}z} + |b_{22}| \mathrm{Li}_{2p}(z). \tag{5}$$

Note, that a singularity at z_s can only occur if the first derivative of the emission profile $\mathrm{d}\mathrm{Li}_{2p}(z)/\mathrm{d}z$ is negative. Therefore the method described above for density evaluation does not run into difficulties as long as $\mathrm{d}\mathrm{Li}_{2p}(z)/\mathrm{d}z \geqslant 0$. The physical interpretation of this singularity is as follows. At small z values the Li(2p) state is mainly populated by excitation from the Li(2s) ground state. If the diagnostic beam

becomes increasingly attenuated with larger z, the depopulation rate for Li(2p) especially due to electron capture by protons will become more important. Finally at z_s the population and depopulation rates due to collisional processes just cancel each other, and the net depopulation of the Li(2p) state will be only due to spontaneous radiative decay.

The proportionality constant α [cf. equations (3) and (4)] can be determined, if this singularity appears between $z = 0$ and z_L, by requiring both the numerator and denominator to change sign at the same value of z. In first approximation the numerator of equation (4) is independent of α, as can be seen from equation (5). The denominator, however, is very sensitive to a variation of α. "Shooting" for a solution means to perform integrations of the rate equations with different values for α until the above requirement is fulfilled. In this way the appearance of a point of singularity can be utilized to calibrate only relatively measured Li(2s–2p) emission profiles. Figure 2 shows density profiles reconstructed from the simulated $\mathrm{Li}_{2p}(z)$ profile of Fig. 1, multiplied by different factors α. Density profiles evaluated with only slightly different factors of α differ strongly from each other in the vicinity of the point of singularity, cf. Fig. 2. This typical behaviour is used to determine a coordinate z_{trans} where reconstruction of the density profile with the one-step method is stopped in good time before appearance of the singularity will cause severe numerical uncertainties.

If no point of singularity occurs in the whole integration range, the unknown factor α is determined by additionally introducing the boundary condition, equation (6).

$$N_1(z_{\mathrm{end}}) = 0 \tag{6}$$

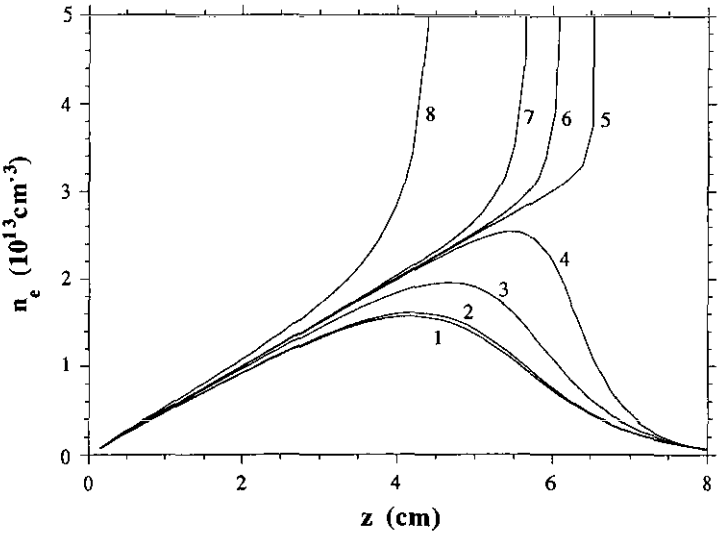

FIG. 2.—Reconstructed electron density from the Li(2p) profile shown in Fig. 1 multiplied by different factors α (cf. text). $\alpha = 1$ gives a linearly increasing electron density (cf. Fig. 1). Numbered curves correspond to various values of α. (1) $\alpha = 0.94596$; (2) $\alpha = 0.95118$; (3) $\alpha = 0.98289$; (4) $\alpha = 0.99915$; (5) $\alpha = 1.00053$; (6) $\alpha = 1.00098$; (7) $\alpha = 1.00344$; (8) $\alpha = 1.05416$.

with z_{end} being the position for vanishing LiI emission profile (more accurately where the LiI intensity $<0.1\%$ of the peak value of its intensity). α is then found by means of the shooting method and fulfilling both boundary conditions, equations (1b) and (6).

For typical TEXTOR discharges, singularities occur where the density reaches approximately several 10^{13} cm^{-3}.

If the one-step method of density evaluation during integration of the rate equations has to be terminated at z_{trans} ($z_{trans} < z_s$) in the vicinity of a singularity, the much more complex multi-step method must be applied for $z > z_{trans}$. This method can only be used when $dLi_{2p}(z)/dz \leqslant 0$ and involves considerably more numerical efforts, but permits density regimes up to 10^{14} cm^{-3} to be reached. Instead of a detailed description of this method, which will be given elsewhere, we just present a reconstruction of the density profile shown in Fig. 1 from the calculated $Li_{2p}(z)$ emission profile of Fig. 1. Comparison of the reconstructed electron density profile with the original one shows excellent agreement as long as the occupation number N_1 for ground state Li atoms remains above 0.1.

In order to demonstrate that this method can fully reconstruct even "pathological" electron density profiles (although the structures appear to be partially smeared out by state-lifetime effects discussed in Section 1) we present in Fig. 3 an arbitrarily structured electron density profile $n_e^{in}(z)$ together with the related (i.e. simulated) $Li_{2p}(z)$ emission profile, and compare it to the reconstructed electron density profile. This comparison shows that spatial variations of the electron density are satisfactorily reproduced and numerical errors involved in our reconstruction method stay small.

If impurities are taken into account, equation (1a) is extended to

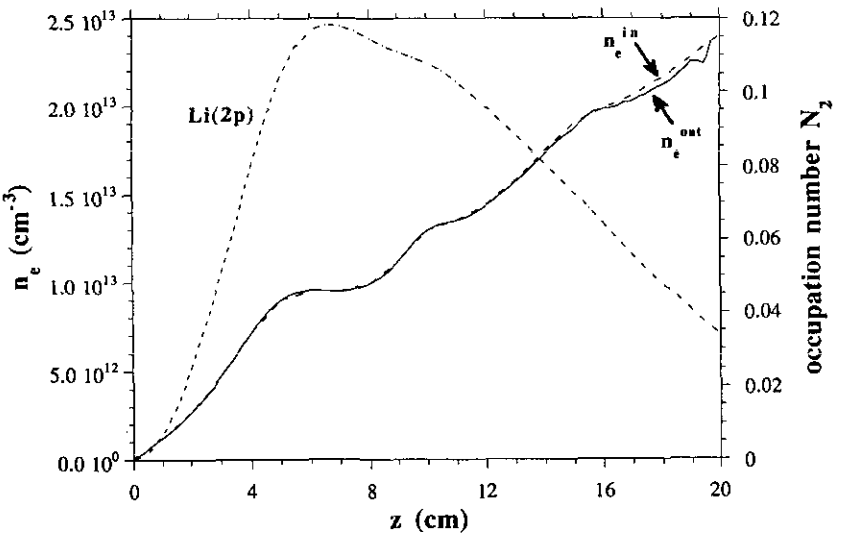

FIG. 3.—Comparison of an arbitrarily structured electron density n_e^{in} with electron density n_e^{out} reconstructed from the corresponding Li(2p) profile.

$$\frac{dN_i(z)}{dz} = (n_e(z)a_{ij}^e(T(z)) + n_p(z)a_{ij}^p(T(z)) + n_Z(z)a_{ij}^Z(T(z)) + b_{ij})N_j(z). \quad (7)$$

We here made use of the effective charge number Z_{eff}

$$Z_{eff} \equiv \frac{n_i q_i^2}{n_e} \quad \text{with} \quad n_e = n_i q_i \quad (8)$$

where we sum over all ion species i with charge q_i and density n_i.

With a given average $q(z)$-profile in combination with a model $Z_{eff}(z)$-profile and quasi-neutrality still valid, the densities n_p and n_Z of protons and impurity ions, respectively can again be expressed in terms of n_e.

$$n_Z = f(z) \cdot n_e(z) \quad (9a)$$

$$n_p(z) = (1 - q(z) \cdot f(z)) \cdot n_e(z) \quad (9b)$$

with $f(z)$ depending on $q(z)$ and $Z_{eff}(z)$.

Inserting equations (9a) and (b) into equation (7) leads to (1a) with different matrix coefficients a_{ij}, by which the impurity distributions as well as the relevant rate coefficients are taken into account. While cross-sections for electron capture from Li into impurity ions have been estimated from the classical over barrier model (RYUFUKU *et al.*, 1980), rate coefficients for all other impurity ion–Li collision processes were derived by q^2-scaling of the respective values for proton–Li collisions.

3. EXPERIMENTAL RESULTS

The above described reconstruction methods have been applied to determine electron density profiles in the edge plasma of the Tokamak experiment TEXTOR at KFA Jülich. The Li injector for TEXTOR is capable of producing neutral lithium beams of 20–30 keV energy and 5–10 mA equivalent current at the plasma boundary, the beam diameter being about 40 mm at this location (SCHORN *et al.*, 1991). The beam enters the TEXTOR plasma radially in the equatorial midplane of the torus.

The LiI 670.8 nm signal resulting from excitation of injected Li atoms in collisions with plasma particles is measured spatially and temporally resolved by means of a large aperture scanning optical detection system. Time resolution in this experiment is currently limited due to a scanning frequency of less than 5 Hz (SCHORN *et al.*, 1991). The spatial resolution amounts to 4 mm in radial orientation. To discriminate the signal from background radiation, the beam is usually chopped with a frequency of 250 Hz. The raw data measured by the optical detection system are first corrected for background and sometimes averaged over a certain time period. Then the data are multiplied by a correction function obtained from LiI profile measurements during injection of the Li diagnostic beam into the TEXTOR vessel filled with low pressure (10^{-5} mbar) H_2 gas. Under these single collision conditions no appreciable attenuation of the beam takes place (which was checked by testing the linearity of the signal intensity on filling pressure), and the obtained radial "apparatus" profile contains the radial dependence of all calibration quantities, e.g. solid angle changing along the beam path, transmission curve of the LiI interference filter (different viewing angle...

different Doppler shift), vignetting due to apertures in the scanning observation system, etc. After these corrections of the raw data, a factor α no longer dependent on radius remains as a proportionality constant in equation (3).

More details about the experimental setup may be found in SCHORN *et al.* (1991) and BAY *et al.* (1986, 1987).

A typical measured radial LiI 670.8 nm emission profile is shown in Fig. 4 (shot #45378). The corresponding electron density as evaluated with the above described methods is presented in Fig. 5. Note the pronounced radial structures in electron density in the vicinity of the ALTII limiter position as compared to the almost structureless LiI emission profile in Fig. 4.

Good agreement in regard to both shape and absolute magnitude is found when we compare the present result with an independent measurement by means of the HCN laser interferometer (SOLTWISCH, 1989) and the laser ablated superthermal Li beam (POSPIESZCZYK and ROSS, 1988a, b) installed at TEXTOR (Fig. 5). Minor discrepancies can be attributed to the different toroidal positions of the diagnostic systems and also to the fact that the spatial resolution of the HCN diagnostics is rather limited because data have to be obtained from Abel inversions of line-averaged electron densities measured at nine discrete radial positions only, the two outermost being located at $r = 40$ and $r = 47.5$ cm, respectively.

With this reconstructed electron density the occupation number N_2 can be modelled as described by SCHORN *et al.* (1991), giving perfect agreement with the experimentally observed LiI emission profile. This comparison has been shown in Fig. 4.

There are basically three factors which may affect the accuracy of the determined density profiles.

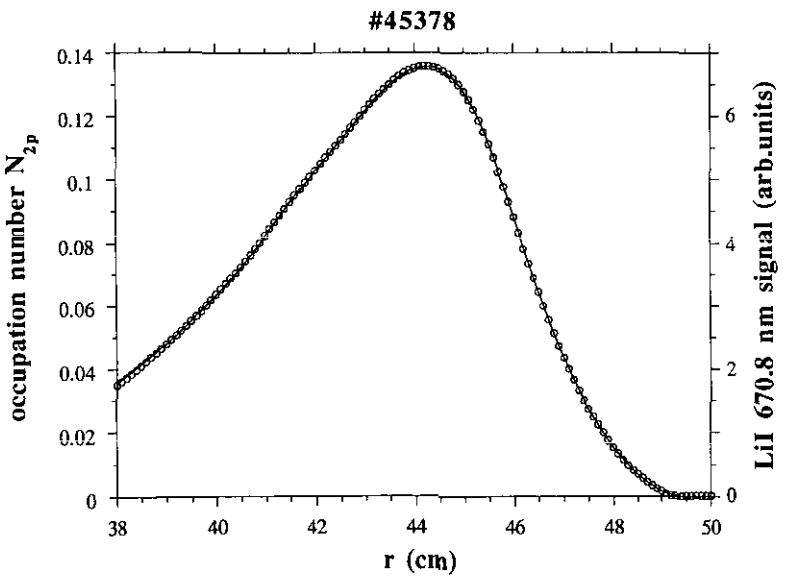

FIG. 4.—Typical radial LiI 670.8 nm emission profile measured with 20 keV Li beam diagnostics for an Ohmically heated TEXTOR discharge #45378 (open symbols) compared with the Li(2p) profile (solid line) as derived from electron density reconstruction by means of the measured profile (see Fig. 5).

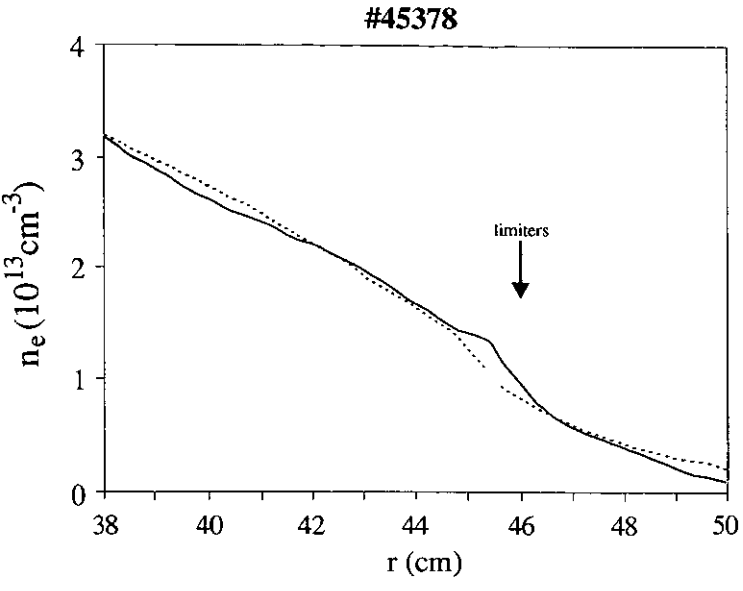

FIG. 5.—Plasma electron density reconstructed from the Li(2p) emission profile as shown in Fig. 4 (solid line), compared with electron densities derived from TEXTOR HCN diagnostics (dotted line for $r < 45$ cm) and density measurements with superthermal laser-ablated Li beam (within the scrape-off layer, dotted line for $r > 45$ cm). The shaded area indicates the error in the reconstructed electron density due to experimental uncertainties (for further explanations, cf. text).

- The main error of the evaluated electron density profile results from the inaccuracy of the applied atomic data base. Except for the Li(2s) ground state atoms, there exist practically no measured cross-sections for the excitation, ionization and electron capture processes. Consequently, available semi-empirical cross-section formulae had to be critically evaluated (SCHNEIDER, 1990). This error source is estimated to yield an uncertainty of about $\pm 20\%$ in absolute n_e magnitude, but only a few percent in the relative radial density profile.
- Experimental inaccuracies in measuring the LiI emission line intensity along the injected Li beam provide the dominant error contribution to the relative radial n_e dependence. We can estimate this contribution by superimposing artificial noise onto the measured signal and applying our reconstruction method. The shaded area in Fig. 5 gives a reasonable estimate for the accuracy of the obtained n_e curve.
- Compared to the two error sources just discussed, the numerical error of our reconstruction method is negligibly small (cf. Fig. 4).

Electron density profiles measured at TEXTOR before and during neutral heating beam injection are presented in Fig. 6. Data have been taken during four different time intervals (Δt_1–Δt_4) of shot #47632. Δt_1 corresponds to the Ohmically heated starting phase of the discharge, after which co-injection with a 1.8 MW deuterium heating beam sets in (Δt_2). During Δt_3 a counter-injection of another deuterium heating beam (1.8 MW) is being added, followed again by co-injection only (Δt_4).

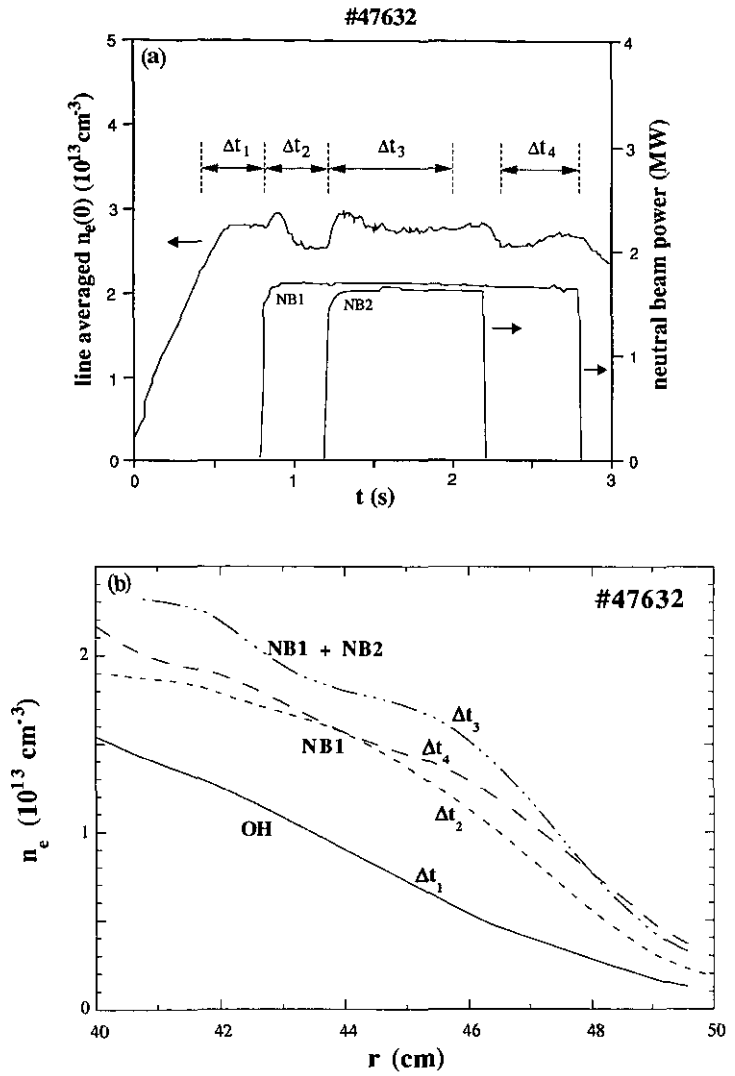

FIG. 6.—(a) Line averaged electron density for TEXTOR discharge #47632 vs time, together with neutral beam power for co- and counter-injector (deuterium heating beams: NB1 and NB2). Four time intervals are indicated, during which LiI-profiles have been measured. (b) Reconstructed electron densities corresponding to time intervals as shown in Fig. 6a.

The central line-averaged electron density as measured by HCN interferometry during the 3 s discharge duration is shown in Fig. 6a together with the neutral beam power and the time intervals during which the LiI profiles have been taken. Resulting electron density profiles are shown in Fig. 6b. During the OH phase the electron density stays comparably low and shows no pronounced structures. Neutral beam heating dramatically increases the edge density and introduces structures in its spatial dependence (CONRADS *et al.*, 1992). Interpretation of this remarkable behaviour will be the subject of future efforts.

4. SUMMARY

We have successfully developed a recursive method for complete reconstruction of the plasma electron density with excellent spatial resolution from scans of the relative LiI 670.8 nm emission intensity along an injected fast Li^0 probing beam. The treatment of beam–plasma interaction includes all relevant collision mechanisms of Li atoms with electrons and plasma ions. Examples of such obtained edge plasma electron density profiles measured at the Tokamak experiment TEXTOR at KFA Jülich have been presented and demonstrate the capability of the new algorithm.

Acknowledgement—Participation of the TU Wien group has been supported by Kommission zur Koordination der Kernfusionsforschung at the Austrian Academy of Sciences.

REFERENCES

AUMAYR F. and WINTER H. (1985) *Ann. Physik* (Leipzig) **42**, 228.
BAY H. L., DULLNI E. and LEISMANN P. (1986) KFA-Report Jül-2062.
BAY H. L., HINTZ E., LEISMANN P., RUSBÜLDT D., AUMAYR F. and WINTER H. (1987) *Proc. 14th European Conf. on Controlled Fusion Plasma Physics*, Madrid, p. 1276 and KFA-Report Jül-2139.
CONRADS H. *et al.*, to be published (1992)
IGUCHI H., KADOTA K., TAKASUGI K., SHOJI T., HOSOKAWA M., FUJWARA M. and IKEGAMI H. (1985) *Rev. Sci. Instrum.* **56**, 1050.
KADOTA K., MATSUNAGA K., IGUCHI H., FUJIWARA M., TSUCHIDA K. and FUJITA J. (1982) *Jpn. J. Appl. Phys.* **21**, L260.
MCCORMICK K., MURMANN H., EL SHAER M. and The ASDEX and NI team (1984) *J. Nucl. Mater.* **121**, 48.
MCCORMICK K. and The ASDEX team (1985) *Rev. Sci. Instrum.* **56**, 1063.
NAG (1984) Numerical Algorithm Group library manual. Downers Grove, Illinois, U.S.A.
POSPIESZCZYK A., AUMAYR F., BAY H. L., HINTZ E., LEISMANN P., LIE Y. T., ROSS G. G., RUSBÜLDT D., SCHORN R. P., SCHWEER B. and WINTER H. (1989) *J. Nucl. Mater.* **162–164**, 574.
POSPIESZCZYK A. and ROSS G. G. (1988a) *Rev. Sci. Instrum.* **59**, 605.
POSPIESZCZYK A. and ROSS G. G. (1988b) *Rev. Sci. Instrum.* **59**, 1491.
RYUFUKU H., SASAKI K. and WATANABE T. (1980) *Phys. Rev. A* **21**, 745.
SCHNEIDER M. (1990) Diplomarbeit TU Wien (unpublished).
SCHORN R. P., HINTZ E., RUSBÜLDT D., AUMAYR F., SCHNEIDER M., UNTERREITER E. and WINTER H. (1991) *Appl. Phys. B* **52**, 71.
SCHORN R. P., WOLFRUM E., AUMAYR F., HINTZ E., RUSBÜLDT D. and WINTER H. (1992) *Nucl. Fusion*, in print.
SOLTWISCH H. (1989) *Phys. Blätter* **45**, 225.
WIESE W. L., SMITH M. W. and MILES B. M. (1969) *Atomic Transition Probabilities*, Vol. II, NSRDS-NBS 22. U.S.A. National Bureau of Standards, Washington DC.